JOURNAL OF CHEMICAL INFORMATION AND MODELING

ARTICLE

pubs.acs.org/jcim

Study of Tamiflu Sensitivity to Variants of A/H5N1 Virus Using Different Force Fields

Trang Truc Nguyen,[†] Binh Khanh Mai,[†] and Mai Suan Li[*,‡]

[†]Institute for Computational Science and Technology, Quarter 6, Linh Trung Ward, Thu Duc District, Ho Chi Minh City, Vietnam

[‡]Institute of Physics, Polish Academy of Sciences, Al. Lotnikow 32/46, 02-668 Warsaw, Poland

Supporting Information

ABSTRACT: An accurate estimation of binding free energy of a ligand to receptor ΔG_{bind} is one of the most important problems in drug design. The success of solution of this problem is expected to depend on force fields used for modeling a ligand−receptor complex. In this paper, we consider the impact of four main force fields, AMBER99SB, CHARMM27, GROMOS96 43a1, and OPLS-AA/L, on the binding affinity of Oseltamivir carboxylate to the wild-type and Y252H, N294S, and H274Y mutants of glycoprotein neuraminidase from the pandemic A/H5N1 virus. Having used the molecular mechanic-Poisson−Boltzmann surface area method, we have shown that ΔG_{bind}, obtained by AMBER99SB, OPLS-AA/L, and CHARMM27, shows the high correlation with the available experimental data. They correctly capture the binding ranking Y252H → WT → N294S → H274Y observed in experiments (Collins, P. J. et al. *Nature* **2008**, *453*, 1258). In terms of absolute values of binding scores, results obtained by AMBER99SB are in the nearest range with experiments, while OPLS-AA/L, which is applied to study binding of Oseltamivir to the influenza virus for the first time, gives rather big negative values for ΔG_{bind}. GROMOS96 43a1 provides a lower correlation as it supports Oseltamivir to be more resistant to N294S than H274Y. Our study suggests that force fields have pronounced influence on theoretical estimations of binding free energy of a ligand to receptor. The effect of all-atom models on dynamics of the binding pocket as well as on the hydrogen-bond network between Oseltamivir and receptors is studied in detail. The hydrogen network, obtained by GROMOS, is weakest among four studied force fields.

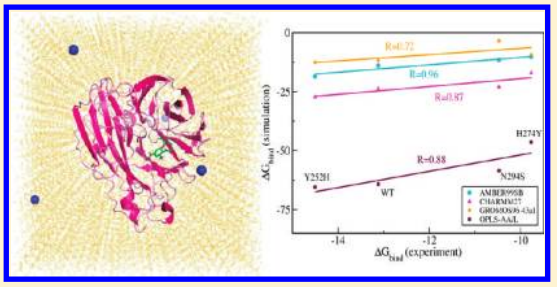

INTRODUCTION

Nowadays the computer-aided drug design approach becomes one of the most useful tools for predicting potential leads for treatment of many diseases. The central problem of this approach is an accurate estimation of the binding free energy ΔG_{bind} which defines the binding affinity of ligand to receptor. The binding affinity is usually studied by the molecular dynamics (MD) and molecular docking simulations. Each of these approaches has its advantages and disadvantages. Docking results provide the information about the location of binding sites and useful insights into the nature of various contributions to the total binding energy (in the context of binding Tamiflu to influenza H5N1 neuraminidase (NA), see refs 1−10), but the predictive docking power is limited. MD simulations are computationally more expensive, but they are more accurate in the estimation of binding free energies.

Results obtained for ΔG_{bind} by MD simulations presumably depend on the methods and the force fields we use. A variety of methods, such as free energy perturbation (FEP),[11] thermodynamic integration (TI),[12] linear interaction energy (LIE),[13] linear response approximation (LRA),[14,15] and molecular mechanic-Poisson−Boltzmann surface area (MM-PBSA),[16] have been used not only for interpretation of existing experimental data but also for prediction. Each method should be considered carefully since it compromises between CPU time efficiency and accuracy level.

In MD simulations one employs force fields which control forces responsible for atomic motion.[17] Force fields are given in the form of empirical potential energy functions and have been developed by different groups. Today OPLS, CHARMM, AMBER, and GROMOS are the most popular force fields. In terms of protein and peptide simulations, a detailed description and comparison among them have been carried out.[18,19] All of force fields have similar functional forms to describe specific interactions but being different significantly with respect to van der Walls (vdW) interaction and partial charges responsible for electrostatic one.[18] Since each force field has been designed to capture a specific type of biological system, its validation for different systems has raised a challenge that should be justified by comparison between simulation results and experimental data.

The question we ask in this paper is how does the binding affinity of Oseltamivir (Tamiflu) to the wild type (WT) and its Y252H, N294S and H274Y mutants of membrane glycoprotein NA from the pandemic A/H5N1 virus depend on force fields. The choice of our research objective is dictated by several reasons. First, the potential impact of pandemic influenza A virus, subtype H5N1, causing great damage to live poultry markets,[20] especially being recognized as a human transmitted

Received: February 14, 2011
Published: August 12, 2011

dx.doi.org/10.1021/ci2000743 | *J. Chem. Inf. Model.* 2011, 51, 2266–2276

virus, has prompted immediate studies to minimize its consequences as much as possible.[21] NA inhibitors Tamiflu and zanamivir (Relenza), which are designed to resemble NA's natural agonist sialic acid, are used for human treatment,[22] but isolates of virus with point mutation in NA may reduce Tamiflu susceptibility.[23,24] Therefore it is important to understand how drug resistant cases are formed in order to provide newly improved therapies. Second, the binding free energies of Tamiflu to WT and variants of NA have been obtained experimentally,[25] and this gives us the opportunity to compare theoretical estimates with the experimental ones. Third, ΔG_{bind} has been computed by different methods and force fields, but a systematic analysis of the role of force fields has not been carried out yet. For example, the MM-PBSA and AMBER package was employed to study the Tamiflu resistant level and explained possible mechanisms of mutant points in A/H5N1 virus.[26−30] CHARMM implemented in NAMD package has been utilized to filter potential drugs.[31,32] Recently, the efficiency of GROMOS and AMBER for studying the impact of calcium on binding of Tamiflu to WT of NA from A/H5N1 virus has been examined.[33] Fourth, the ability of OPLS-AA/L to describe the binding affinity of Tamiflu and its variants have not been probed yet. Finally, ΔG_{bind} of Tamiflu to mutant Y252H has not been computed theoretically.

Using the MM-PBSA method and four force fields GROMOS96 43a1,[34] OPLS-AA/L,[35] AMBER99SB,[36] and CHARMM27,[37] we have computed the binding free energy of Tamiflu to WT and three mutants Y252H, N294S and H274Y of NA. It should be noted that GROMOS96 43a1, OPLS-AA/L, and CHARMM27 are chosen because they are often used to study the drug−protein interaction. The AMBER 03 is more recent than AMBER99SB, but we prefer the latter because the former provides worse results for the binding free energy of Tamiflu to WT (see Figure 4 below). Results obtained by four force fields are compared with experiments to shed light on reliability of each force field. The OPLS-AA, AMBER99SB, and CHARMM27 force fields display a rather high correlation with experiments because they correctly mimic the binding ranking Y252H → WT → N294S → H274Y. Among them, AMBER is the best one because it gives the binding free energies that are in the nearest range with experiments. The values of ΔG_{bind} provided by OPLS are far below the experimental ones. GROMOS displays the lowest correlation, as it indicates that N294S, not H274Y, is the most sensitive to NA. Moreover, due to the united-atom approximation, GROMOS generates configurations which are less stable during the MD course compared with other all-atom models. The hydrogen-bond (HB) network between Oseltamivir and all receptors was found to be weakest in GROMOS. Within all studied force fields we have shown that, in accordance with the experiment,[25] the Y252H mutant displays higher binding affinity than other variants.

MATERIALS AND METHODS

Crystal Structures of WT and Mutants of NA from A/H5N1 Complexed with Tamiflu. The initial structures of A/H5N1 WT and mutants H274Y and N294S were obtained from Protein Data Bank with PDB ID 2HU4, 3CL0, and 3CL2, respectively.[25] Y252H was derived by the corresponding mutation in WT structure using the Mutagenesis module, integrated in PyMOL package.[38] Tamiflu's charges and atom types for the united-atom GROMOS96 43a1 force field were parametrized by Dundee PRODRG2.5 Server (Beta).[39] For the remaining all-atom force fields, atomic partial charges for Tamiflu were derived by electrostatic potential (ESP) charge. To obtain minimized geometries for electrostatic potential calculations, its geometries were first optimized with Gaussian98[40] using the B3LYP/6-31G* level of theory. Fitting charges to the electrostatic potential was subsequently done by the restrained electrostatic potential (RESP) method.[41] Hartree−Fock (HF)/6-31G(d) level of theory is used in the parametrization of the AMBER force field because it overpolarizes the solute, taking implicitly into the account the solvent polarization effects.[42,43] We have used this method to recalculate partial atomic charges, but they do not deviate much from the B3LYP results (Figure S1, Supporting Information). Atom types for Tamiflu were derived from different modules to get along with each force field. For example, ACPYPE[44] and MKTOP[45] were adjusted to provide suitable atom types in the OPLS-AA/L[35] force field. In AMBER99SB and CHARMM27,[37] atom types were named by ACPYPE and SwissParam,[46] respectively. The atom types and EPS atomic charges of Tamiflu are collected in Supporting Information for four force fields (Tables S1−S4).

Molecular Dynamic Simulations. Complexes of NA−Tamiflu were placed in a triclinic box of about 11 400 water molecules with 1 nm distance between the solute and the box (a typical snapshot is shown in Figure S2, Supporting Information). In the united-atom model, the receptor and the ligand have 3832 (5749), 3826 (5745), 3829 (5746), and 3838 (5753) atoms for WT, Y252H, N294S, and H274, respectively. The numbers in parentheses refer to all-atom models. The periodic boundary condition is imposed with 1.4 and 1.0 nm cutoff for vdW and electrostatic interactions. The long-range electrostatic interaction is computed by the particle-mesh Ewald summation method.[47] Equations of motion were integrated using a leapfrog algorithm[48] with a time step 1 fs. The nonbonded interaction pair−list was updated every 10 fs with the cutoff of 1 nm. To neutralize WT, Y252H, and N294S systems, four NA^+ ions were added, while for H274Y, one adds two NA^+ ions (Figure S2, Supporting Information). Then the systems are minimized to remove not only bad van der Waals contacts with water but also the local strain in the protein that appears during addition of hydrogen atoms. By applying the conjugate gradient method every 50 steps of steepest descent, the minimization is converged when the maximum force becomes smaller than 0.01 kJ/mol/nm. Then, atoms of protein were restrained, leaving the rest to be relaxed for 100 ps in order to obtain evenly distributed systems. The temperature was gradually heated to 300 K during 100 ps with 5 kcal/mol harmonic restraints in all systems. The equilibration was next performed coupling with temperature and pressure. Constant temperature 300 K was enforced using Berendsen algorithm[49] under 50 ps constant volume and temperature (NVT) simulation with a damping coefficient of 0.1 ps. We used the Parrinello−Rahman pressure coupling[50] in 100 ps constant pressure and temperature (NPT) run at 1 atm constant pressure with the damping coefficient of 0.5 ps. The final NPT simulations of 20 ns were carried out with an 1 fs time step. We have used Gromacs-4.5 package[51] to run the MD simulations with four force fields. Our choice of the water model for each force field has been made following the recommendation of this package. Namely, the simple point charge (SPC)[52] water model is chosen for the GROMOS, while TIP4P[53] is for OPLS. TIP3P[53] is recommended as the most suitable for AMBER and CHARMM.

Binding Free Energy Calculation by MM-PBSA. The binding free energy is defined as follows:

$$\Delta G_{bind} = G_{complex} - G_{free\text{-}protein} - G_{free\text{-}ligand} \quad (1)$$

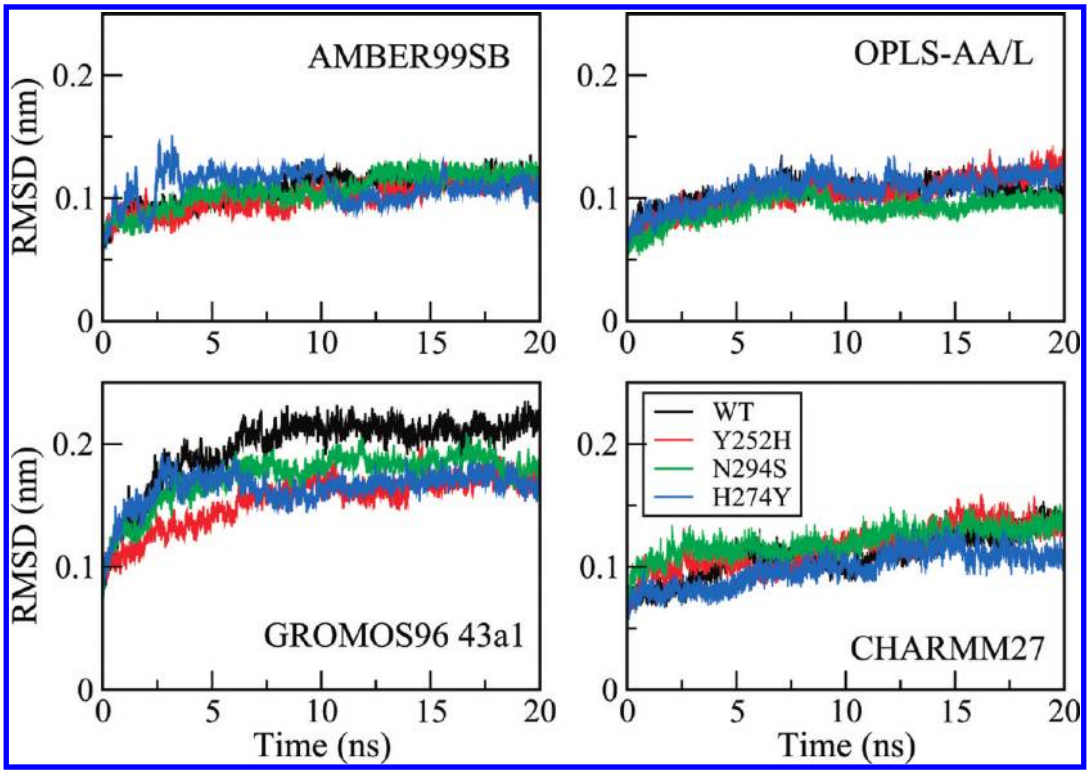

Figure 1. Time dependence of the backbone RMSD of WT (black), Y252H (red), N294S (green), and H274Y (blue) of A/H5N1 NA. Results are shown for four force fields. Arrows roughly refer to times when systems reach equilibrium.

In the MM-PBSA, the free energy of each molecule is given by the following equation:

$$G = E_{mm} + G_{solvation} - TS \quad (2)$$

To incorporate all possible nonbonded interactions, the molecular mechanics energy of the solute in the gas phase E_{mm} was computed for each snapshot with no cut-offs:

$$E_{mm} = E_{bond} + E_{angle} + E_{torsion} + E_{elec} + E_{vdW} \quad (3)$$

The intramolecular electrostatic (E_{elec}) and vdW (E_{vdW}) interaction energies are calculated by the Gromacs utility with the same force field used in MD simulations.

The free energy of solvation, $G_{solvation}$, was approximated as the sum of electrostatic and nonpolar contributions:

$$G_{solvation} = G_{PB} + G_{sur} \quad (4)$$

Here G_{PB} derived from the electrostatic potential between solute and solvent was determined using the continuum solvent approximation.[54] It is the change of electrostatic energy from transferring solute in a continuum medium, from a low solute dielectric constant ($\varepsilon = 2$) to a higher one with water without salt ($\varepsilon = 78.45$). Using a grid spacing of 0.1 Å, the APBS package[55] was implemented for numerical solution of the corresponding linear Poisson−Boltzmann equation. The GROMOS radii and charges were used to generate PQR files. Then, the nonpolar solvation term G_{sur} was approximated as linearly dependent on the solvent accessible surface area (SASA), derived from Shrake−Rupley numerical method[56] integrated in the APBS package. $G_{sur} = \gamma SASA + \beta$, where $\gamma = 0.0072$ kcal/mol·Å^2 and $\beta = 0$.[57]

Solute entropy contributions were estimated from the average of three snapshots randomly taken from MD runs. Structures were minimized with no cutoff for nonbonded interactions by using the conjugate gradient and low-memory Broyden−Fletcher−Goldfarb−Shanno method[58] until the maximum force was smaller than 10^{-6} kJ/(mol·nm). The conformational entropy of the solute S, estimated from normal-mode analysis by diagonalizing the mass-weighted Hessian matrix,[59] is as follows:

$$S_{vib} = -R \ln(1 - e^{-\hbar\nu_0/k_BT}) + \frac{N_A \nu_0 e^{-\hbar\nu_0/k_BT}}{T(1 - e^{-\hbar\nu_0/k_BT})} \quad (5)$$

Here S_{vib} is the vibrational entropy, $\hbar$ is Plank's constant, ν_0 is the frequency of the normal mode, k_B is the Boltzmann constant, T is 300 K, and N_A is Avogadro's number. It should be noted that we used snapshots collected every 10 ps in the equilibrium of each system to compute other terms of ΔG_{bind}.

Measures Used in Data Analysis. The root-mean-square deviation (RMSD) is employed to measure the deviation of structures from the initial configuration. We also use the root-mean-square fluctuation (RMSF) to characterize departures of individual atomic positions from the first frame of simulations. The HB is assumed to be formed if the distance between proton donor (D) and proton acceptor (A) is less than 0.35 nm and the angle H−D−A is also less than 30°.

RESULTS AND DISCUSSION

Stability of Simulated Systems. To explore the stability of four complexes of Tamiflu with WT and variants of A/H5N1 virus, their backbone RMSD values relative to the initial structures during 20 ns MD runs are plotted as a function of time (Figure 1). In the CHARMM27 case, all systems reach equilibration after 15 ns, while for remaining force fields, the equilibrium takes place at time scales of 10 ns. RMSD fluctuates slightly

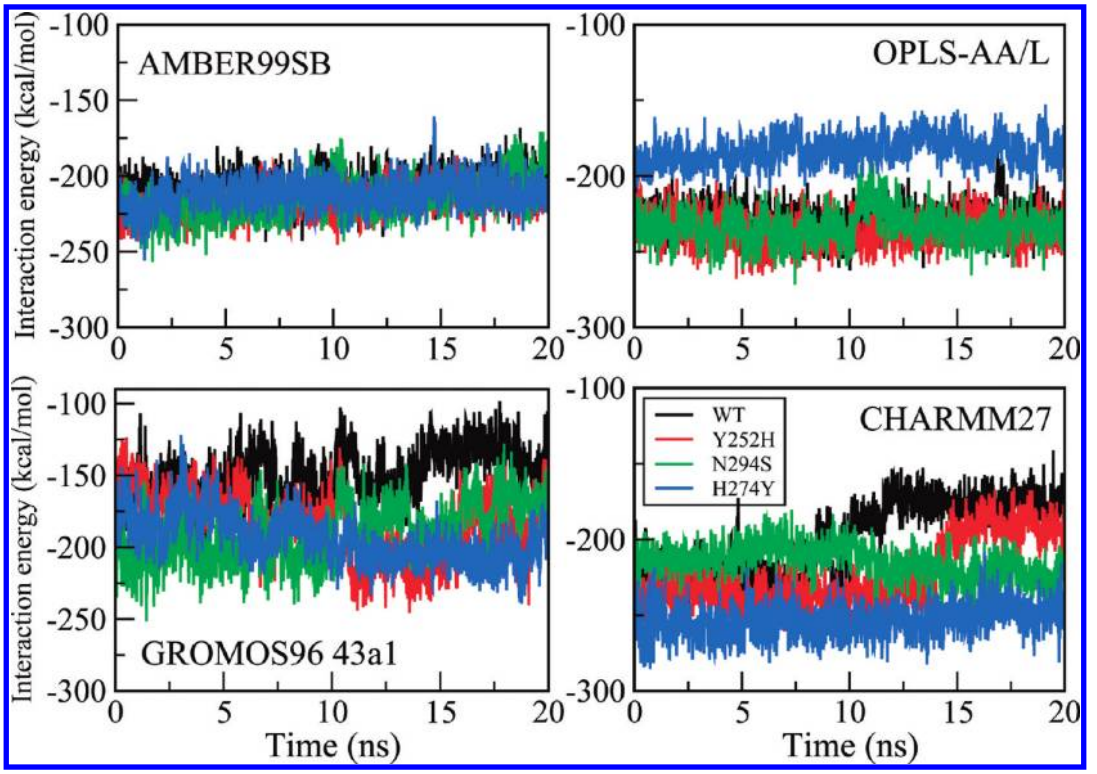

Figure 2. Same as in Figure 1 but for the interaction energies between Tamiflu and receptors. The interaction energy involves the electrostatic and vdW contributions.

Table 1. Binding Free Energies (in kcal/mol) of Tamiflu to WT and Mutants of A/H5N1 NA Calculated by MM-PBSA Method and GROMOS96 43a1 Force Field

	ΔE_{elec}	ΔE_{vdW}	ΔG_{sur}	ΔG_{PB}	$-T\Delta S$	ΔG_{bind}	G_{exp}
WT	−116.24 ± 0.074	−25.03 ± 0.014	−4.22 ± 0.002	120.51 ± 0.074	13.19	**−11.79**	−13.12
Y252H	−166.17 ± 0.076	−28.12 ± 0.013	−4.90 ± 0.002	172.44 ± 0.076	14.26	**−12.49**	−14.50
N294S	−152.14 ± 0.085	−25.41 ± 0.012	−4.72 ± 0.002	163.13 ± 0.084	15.67	**−3.47**	−10.48
H274Y	−177.36 ± 0.086	−27.03 ± 0.011	−4.72 ± 0.002	184.39 ± 0.086	15.46	**−9.26**	−9.77

around 0.1 nm in OPLS-AA/L, AMBER99SB, and CHARMM27, but the GROMOS96 force field provides larger fluctuations of ≈0.2 nm. The higher instability of GROMOS is probably associated to the united-atom approximation, where the total number of atoms is smaller than in other all-atom models. This is also evident from the time dependence of the interaction energies (including vdW and electrostatic terms) between the ligand and the receptor (Figure 2). Within OPLS-AA/L, AMBER99SB, and CHARMM27, they fluctuate to a lesser extent compared to the GROMOS 43a1 force field during whole MD runs. In the equilibrium, systems become stable, and snapshots collected in this period (the last 5 ns for CHARMM and 10 ns for AMBER, OPLS and GROMOS) are used for the MD analysis and MM-PBSA calculation of ΔG_{bind}.

Comparison of Binding Free Energies Obtained by Different Force Fields. *GROMOS96 43a1 Force Field.* In GROMOS96 43a1, the electrostatic energy gained from the complex formation in the gas phase compensates for the loss in polar solvation energy (Table 1). The sum of these terms is always positive (Table 1). The apolar solvation energies and the entropy lost upon binding are almost the same among all complexes. The vdW interaction is also not sensitive to mutations. Experimentally,

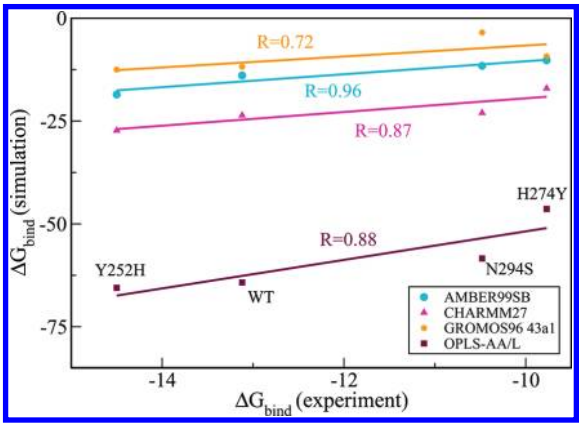

Figure 3. Comparison of theoretically calculated binding free energies with the experimental ones.[25] The correlation level is R = 0.74, 0.77, 0.87, and 0.88 for AMBER99SB (cyan), GROMOS96 43a1 (orange), CHARMM27 (magenta), and OPLS-AA/L (purple), respectively.

mutations H274Y and N294S in the A/H5N1 NA structure lead to 300−1700- and 20−80-fold reductions in Tamiflu sensitivity,

Table 2. Binding Free Energies (in kcal/mol) of Tamiflu to WT and Mutants of A/H5N1 NA Calculated by MM-PBSA Method and OPLS-AA/L Force Field

	ΔE_{elec}	ΔE_{vdW}	ΔG_{sur}	ΔG_{PB}	$-T\Delta S$	ΔG_{bind}	G_{exp}
WT	−208.64 ± 0.105	−20.37 ± 0.011	−4.98 ± 0.002	153.48 ± 0.077	16.26	**−64.25**	−13.12
Y252H	−213.66 ± 0.107	−22.34 ± 0.011	−4.89 ± 0.002	159.86 ± 0.080	15.47	**−65.56**	−14.50
N294S	−209.68 ± 0.105	−21.62 ± 0.011	−5.00 ± 0.002	160.80 ± 0.080	17.10	**−58.40**	−10.48
H274Y	−156.34 ± 0.078	−24.10 ± 0.012	−4.90 ± 0.002	124.67 ± 0.062	14.29	**−46.38**	−9.77

Table 3. Binding Free Energies (in kcal/mol) of Tamiflu to WT and Mutants of A/H5N1 NA Calculated by MM-PBSA Method and AMBER99SB Force Field

	ΔE_{elec}	ΔE_{vdW}	ΔG_{sur}	ΔG_{PB}	$-T\Delta S$	ΔG_{bind}	G_{exp}
WT	−175.67 ± 0.176	−28.98 ± 0.029	−4.96 ± 0.005	181.50 ± 0.182	14.20	**−13.91**	−13.12
Y252H	−184.26 ± 0.125	−29.84 ± 0.035	−5.29 ± 0.005	185.99 ± 0.189	14.86	**−18.54**	−14.50
N294S	−191.01 ± 0.183	−20.07 ± 0.033	−5.22 ± 0.005	189.06 ± 0.176	15.67	**−11.57**	−10.48
H274Y	−181.01 ± 0.164	−22.89 ± 0.031	−5.13 ± 0.004	182.68 ± 0.187	16.11	**−10.24**	−9.77

respectively.[25] Meanwhile, the Y252H substitution which was in the H5N1 virus isolated from infected patients in Vietnam and Cambodia raised the sensitivity by 10-fold.[25] Thus our finding is consistent with the experiment in the sense that N294S and H274Y display more resistance to Tamiflu than to WT (Table 1), while Y252H increases the binding affinity. The best agreement with the experiment has been found for WT and H274Y. However, the large departure from the experimental result observed for ΔG_{bind} of N294S makes the correlation between simulation and experiment not so high (R = 0.72, Figure 3).

Using the GROMOS96 force field and the TI method for WT, Lawrenz et al.[33] obtained $\Delta G_{bind} \approx -10.4$ kcal/mol, which is higher than ours as well as the experimental value. Since authors of ref 33 did not specify what version of GROMOS96 they used, it is difficult to compare with our result from the GROMOS96 43a1 force field. One of possible sources for discrepancy comes from different methods used in estimation of ΔG_{bind}.

OPLS-AA/L Force Field. To our best knowledge, this force field has not been employed to estimate the binding free energy of Tamiflu to NA WT and mutants so far. Our results obtained by OPLS-AA/L and MM-PBSA are shown in Table 2. Contrary to GROMOS, the electrostatic and polar solvation energies of all systems do not compensate each other, resulting in large negative values of the total binding free energies. In terms of absolute binding scores, the departure from experiments is smallest (−4 to −0.5 kcal/mol) in AMBER (see below), while the largest one (−50 to −37 kcal/mol) falls into OPLS.

Although ΔG_{bind} has very large negative values, the correlation with experimental results remains high (R = 0.88, Figure 3). More importantly, this force field correctly reflects the general trend of binding affinities experimentally observed for four systems, Y252H → WT → N294S → H274Y.[25] Due to the strong electrostatic interaction, Tamiflu shows higher binding affinity to Y252H than to WT, having ΔG_{bind} lower by an amount of about 1.31 kcal/mol (Table 2). Thus, both experimental and our theoretical estimations show that Y252H about 15-fold increases susceptibility of Tamiflu to receptor (Table 2). H274Y is the most drug-resistant case not only in OPLS-AA/L but also in AMBER99SB and CHARMM force fields (see below).

AMBER99SB Force Field. AMBER is frequently used by many research groups for studying the binding between Tamiflu and NA in the A/H5N1 virus. According to the amount of vdW energies being lost upon the binding process, one can divide four systems into two groups where Y252H and WT are more susceptible to Tamiflu than N294S and H274Y (Table 3). The sum of electrostatic and polar solvation energies decides the order of binding ranking that Y252H is better than WT and H274Y is worse than N294S upon association with Tamiflu. Thus, similar to OPLS, the AMBER99SB force field exactly captures the binding tendency Y252H → WT → N294S → H274Y. In addition, the values of ΔG_{bind} yielded from AMBER are not only in the nearest range with experiments but also have the highest correlation (R = 0.96) among the four force fields. Thus, this force field is the best one and highly recommended for studying the binding of Tamiflu to influenza virus. Whether this option is good for other systems remains to be elucidated.

CHARMM27 Force Field. As follows from Table 4, for all studied systems the electrostatic and polar solvation contributions do not compensate each other. As in the AMBER and OPLS modeling, CHARMM27 correctly reflects the relative binding affinities of four systems (Table 4), although the values of ΔG_{bind} themselves are lower than experimental ones (from 7 to 12 kcal/mol). The binding free energies of Oseltamivir to WT and N294S do not deviate as much as shown by the experiments,[25] but the tiny difference in ΔG_{bind} still favors WT as a better receptor. Since the relative binding level of four systems estimated by CHARMM27 force field is the same as observed in the experiments, the correlation remains rather high (R = 0.87, Figure 3). Such a good correlation is compatible with the OPLS case (R = 0.88).

Comparison with Other Works. In most of previous studies, the AMBER and MM-PBSA methods have been employed for estimating the binding free energy of Tamiflu to WT in closed conformation (Figure 4). Results reported by different groups profoundly vary from −25.97[28] to −2.18,[26] covering our values ΔG_{bind} = −23.62, −13.91, and −11.79 kcal/mol obtained by CHARMM, AMBER, and GROMOS force fields, respectively. Having used PARMM99 and MM-PBSA, Wang and Zheng[26] even obtained positive values of ΔG_{bind} for H274Y and N294S. This may be associated with their short MD runs of 6 ns.

The binding free energies estimated for WT by LIE and AMBER or CHARMM do not fluctuate much, varying from −11.4[60] to −8.06 kcal/mol[31,32] (see also Figure 3). They are a bit higher than the experimental value −13.12 kcal/mol.[25] Recently,

Table 4. Binding Free Energies (in kcal/mol) of Tamiflu to WT and Mutants of A/H5N1 NA Calculated by MM-PBSA Method and CHARMM27 Force Field

	ΔE_{elec}	ΔE_{vdW}	ΔG_{sur}	ΔG_{PB}	$-T\Delta S$	ΔG_{bind}	G_{exp}
WT	−210.71 ± 0.429	−17.82 ± 0.164	−4.87 ± 0.005	195.15 ± 0.323	14.63	**−23.62**	−13.12
Y252H	−218.97 ± 0.294	−18.68 ± 0.154	−5.01 ± 0.005	201.07 ± 0.181	14.29	**−27.30**	−14.50
N294S	−215.56 ± 0.490	−17.00 ± 0.167	−5.21 ± 0.007	199.19 ± 0.472	15.56	**−23.02**	−10.48
H274Y	−229.96 ± 0.538	−17.75 ± 0.186	−4.93 ± 0.005	220.82 ± 0.369	14.76	**−17.06**	−9.77

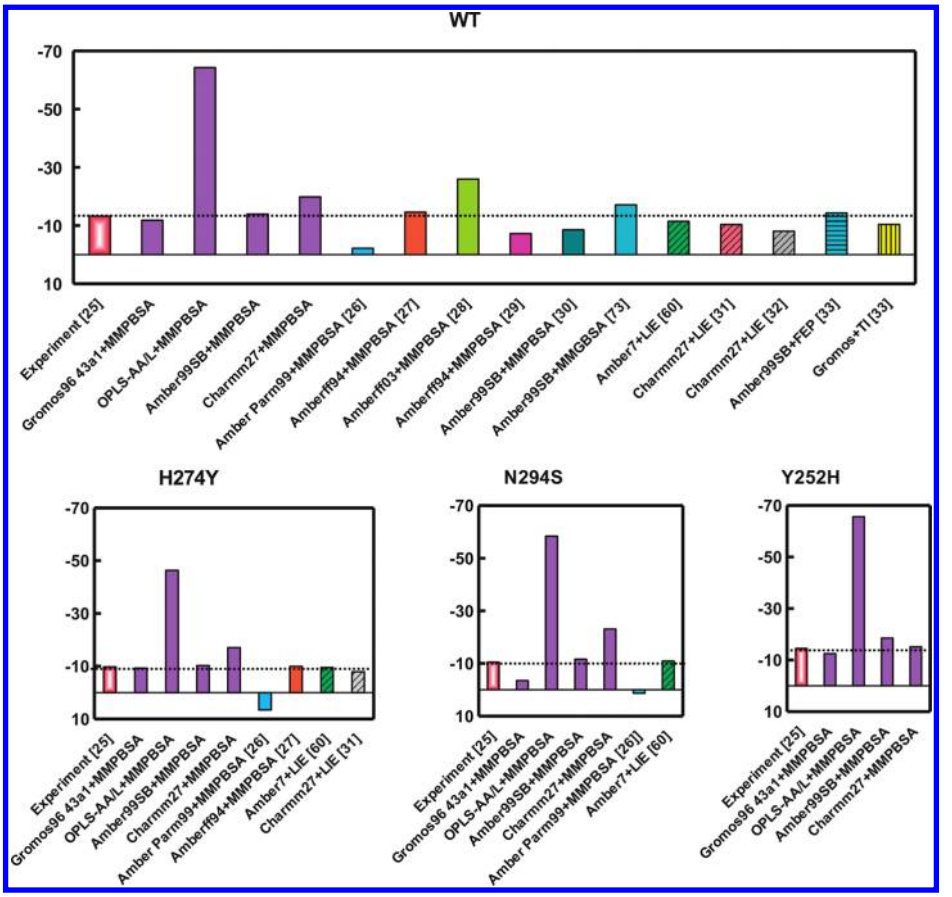

Figure 4. Binding free energies estimated by different force fields and methods. The experimental value[25] is marked by the horizontal line. Violet refers to results obtained in this work. The experimental values of ΔG_{bind} are estimated from the inhibition constants K_i[25,71,72] using the formula $\Delta G_{bind} = RT \ln(K_i)$. Here $R = 1.987 \times 10^{-3}$ kcal/mol, $T = 300$ K, and K_i is measured in M. The AMBER99SB and MM-GBSA methods have been used to obtained ΔG_{bind} for WT.[73]

Lawrenz et al. have reported $\Delta G_{bind} = -14.3$ kcal/mol obtained by AMBER and FEP, while GROMOS and TI give −10.4 kcal/mol.[33] ΔG_{bind} = − 13.91 kcal/mol (Table 3), obtained by AMBER99SB in this work, is the best one as it is closest to the experimental value. OPLS-AA/L provides the big deviation from the experiments and the other theoretical studies by different force fields (Table 2).

Studies of resistance mechanism of H274Y mutant of A/H5N1 to Tamiflu by different groups also lead to different results. ΔG_{bind} obtained by AMBER and MM-PBSA also varies significantly from −9.9[27] to 6.5 kcal/mol[26] (Figure 4), while AMBER and LIE distribute the same range results of −9.5[60] and −7.86 kcal/mol.[31] The results obtained by Malaisree et al.[27] and Rungrotmongkol et al.[60] are in good agreement with the experimental data −9.77 kcal/mol. Our estimations by AMBER and GROMOS (Tables 1 and 3 and Figure 4) also agree with the experiments, while OPLS and CHARMM provide much lower values for ΔG_{bind} (Tables 2 and 3).

In the case of N294S, AMBER7 and LIE give −10.9 kcal/mol[60] which is very close to the experimental finding −10.48 kcal/mol[25] (Figure 4). Having used MM-PBSA and PARMM99, one obtained ΔG_{bind} = 1.35 kcal/mol[26] showing that Tamiflu favors to stay away from the binding pocket of A/H5N1. Our simulations by MM-PBSA and all four force fileds show that, in accordance with the experiment,[25] ΔG_{bind} is negative (Tables 1−4). AMBER99SB provides the best agreement with the experiments, while ΔG_{bind} obtained by OPLS and CHARMM is pronouncedly below the experimental value of −10.48 kcal/mol. Within GROMOS, Tamiflu displays very low binding affinity to N294S having $\Delta G_{bind} = -3.47$ kcal/mol. This result reflects drawbacks of the united-atom approximation.

As mentioned above, mutant Y252H has not been theoretically studied yet. Our MM-PBSA results imply that all force fields

dx.doi.org/10.1021/ci2000743 |J. Chem. Inf. Model. 2011, 51, 2266–2276

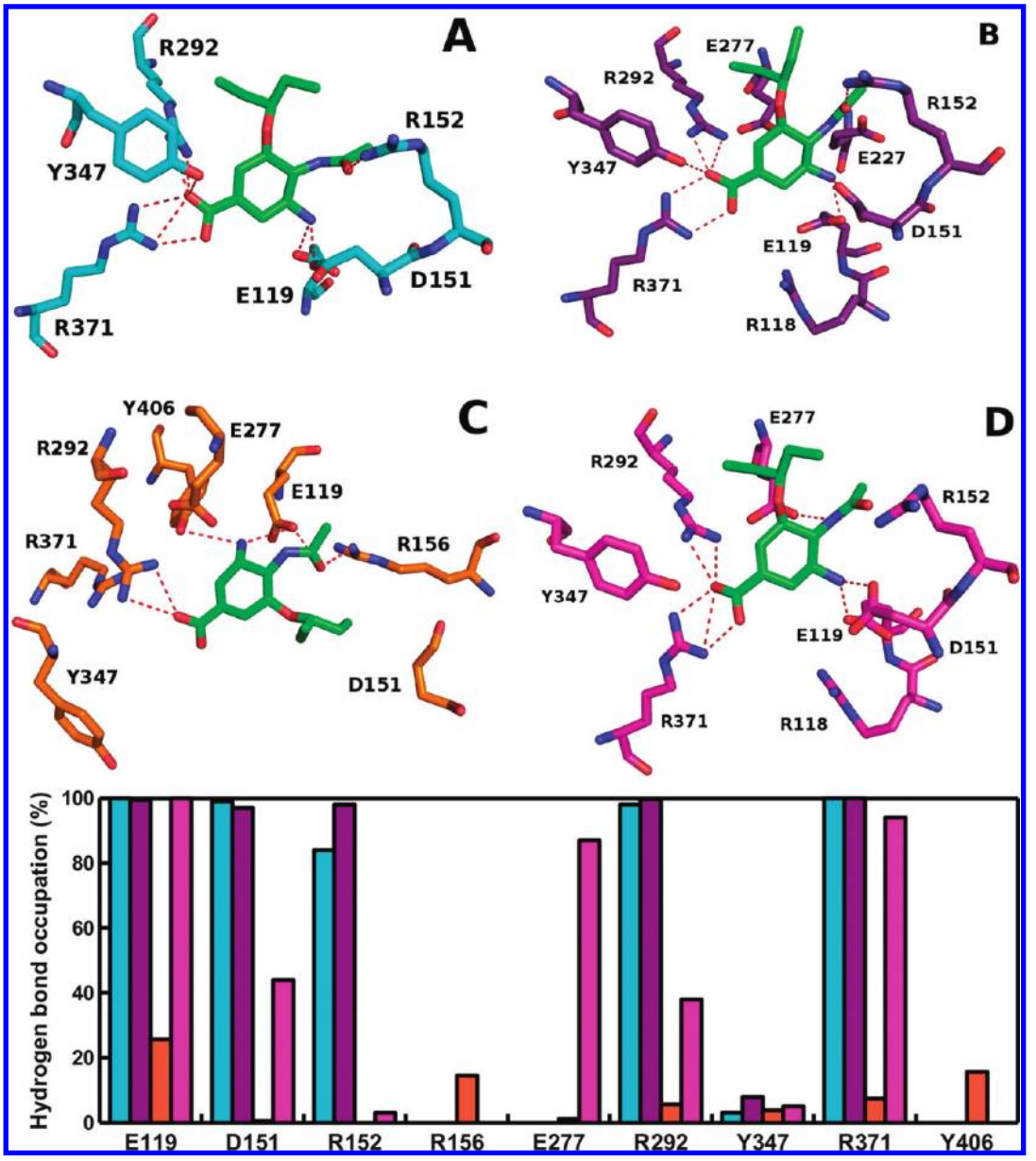

Figure 5. Typical snapshots for the HB network between Tamiflu's charged groups and residues of WT at the binding site obtained by various force fields. HBs are as follows. (A) AMBER99SB: $-COO^-$ and $-NH_2$ (R371,R292), $-OH$ (Y347); $-NH_3^+$ and $-COO^-$(D151,E119); NHAc and $-COO^-$(E277). (B) OPLS-AA/L: $-COO^-$ and $-NH_2$ (R371,R292), $-OH$ (Y347); $-NH_3^+$ and $-COO^-$ (D151,E119); NHAc and $-NH_2$ (R152). (C) GROMOS96 43a1: $-COO^-$ and NH_2 (R152); $-NH_3^+$ and $-COO^-$(E119), $-OH$ (Y406); NHAc and $-COO^-$(E227,E277), $-OH$ (S179). (D) CHARMM27: $-COO^-$ and NH_2 (R371,R292); $-NH_3^+$ and $-COO^-$(D151,E119); NHAc and $-COO^-$(E277). All hydrogen atoms are implicit. Lower panel refers to the probability of formation of HBs between Tamiflu and WT. Results are averaged over the last 2 ns of simulation. Cyan, maroon, orange, and magenta refer to AMBER99SB, OPLS-AA/L, GROMOS96, and CHARMM27, respectively.

are suitable to capture the experimental finding[25] that this mutant is more susceptible to Tamiflu than WT (Figure 4). GROMOS provides the best agreement with the experiment (Table 1), but this result may be accidental.

Effects of Different Force Fields on Receptor−Drug Interaction at the Binding site. *Electrostatic Interaction Is More Important Than vdW.* As follows from Tables 1−4, for all force fields, the Coulomb interaction dominates over the vdW one. This conclusion is consistent with previous theoretical works.[26−28,30,32,33,60] Our new finding is that OPLS-AA/L does not change this conclusion. The dominating role of the electrostatic interaction has been also observed for binding of many ligands to NA of A/H1N1 virus.[61]

The role of the Coulomb interaction for the binding of Tamiflu to WT and mutants depends on force fields. Within GROMOS96 and CHARMM, this interaction is strongest for H274Y (Tables 1 and 4). However, N294S and Y252H show the strongest Coulomb interaction with Oseltamivir in AMBER99SB and OPLS, respectively (Tables 2 and 3). The difference presumably comes from different sets of charges used for different models. ΔE_{vdW} shows the weak force field dependence ranging from −17.00 (Table 4) to −29.84 kcal/mol (Table 3). The electrostatic interaction is mainly compensated by a large positive contribution of ΔG_{PB} which varies across force fields. However, the relation $\Delta G_{PB} < -\Delta E_{elec}$ always holds for CHARMM and OPLS, resulting in large negative values of

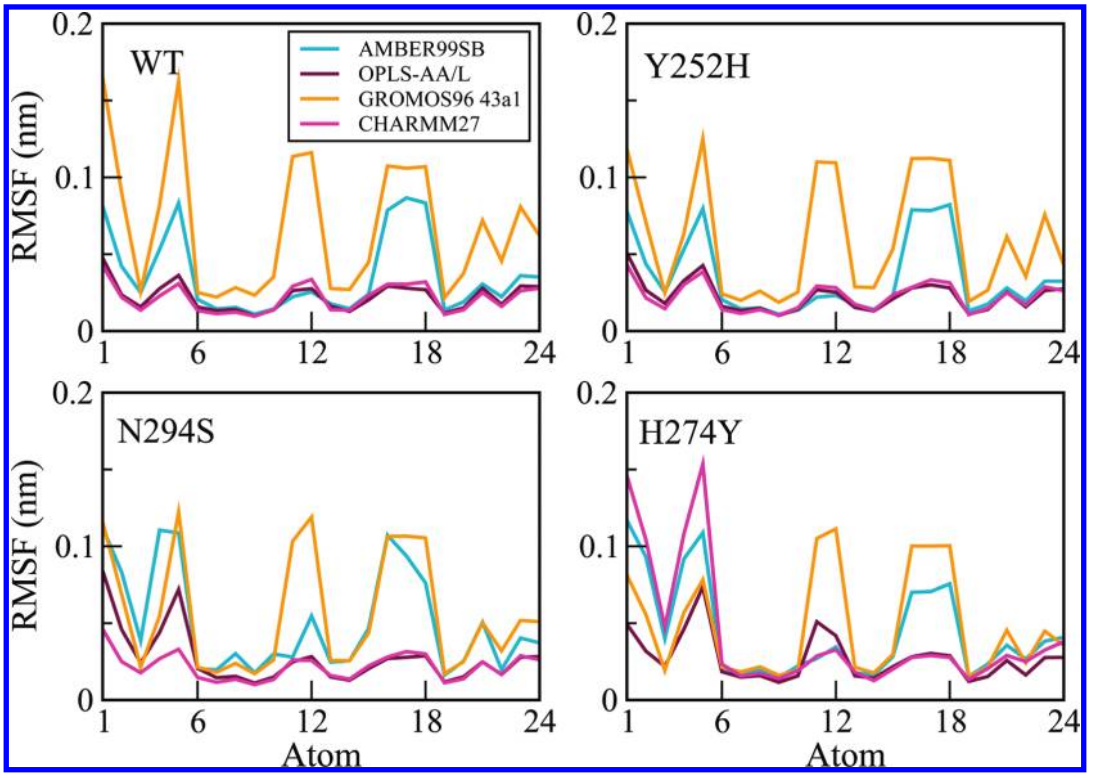

Figure 6. RMSF of individual atoms of Tamiflu in the binding pocket of WT and other variants. Results are averaged over last 2 ns of the simulation with four force fields. Cyan, maroon, orange, and magenta refer to AMBER99SB, OPLS-AA/L, GROMOS96, and CHARMM27, respectively. Atom index of Tamiflu is as follows: 1−6, $-OCHEt_2$; 10−12, −COO; 15−18, $-NH_3^+$; and 19−24, −NHAc.

binding scores. Within GROMOS ΔG_{PB} is always larger than $-\Delta E_{elec}$, while this relationship is not valid for all systems in AMBER modeling.

Nonpolar and Entropic Contributions Are Not Sensitive to Force Fields. As follows from Table 1−4, ΔG_{sur} is about 5 kcal/mol, while $-T\Delta S$ fluctuates between 13 and 17 kcal/mol for all systems and force fields we used. Such a result is not surprising because the ligand is small compared to the receptor and the energy change due to SASA change should be minor. The same argument is applied to the entropy contribution which is small due to tiny ligand conformation variations.

Hydrogen-Bond Network. From MM-PBSA results, the hydrogen bonding, which mostly contributes to the electrostatic energy, plays the key role in the interaction between Tamiflu and all variants of A/H5N1.[29] Figures S3−S6, Supporting Information, show the time dependence of the number of HBs obtained by force force fields for WT, Y252H, N294S, and H274Y, respectively. This number not only levels significantly among force fields but also depends on systems (see also lower panel of Figure 5).

In the WT case, within AMBER99SB, OPLS-AA/L, and CHARMM27, the population of hydrogen bonding between ligand and conserved residues E119 and R371 from the binding pocket exceeds 85%. At D151, R152, and R292, they distribute thoroughly with Tamiflu in CHARMM to a lesser extent compared to AMBER and OPLS (Figure 5). However, HBs mainly distribute between E277 and the ligand in CHARMM. Using MD simulations and the AMBER force field,[62] Udommaneethanakit et al. have shown that the existence of a HB between Tamiflu and residue D151 is directly related to the formation of the close/open conformation of the flexible 150 loop.[63] This observation is consistent with our results. In GROMOS96 force field, the number of HBs is quite low (<10% with R292, Y347, and R371) and at residues R156 and Y406, which do not form HBs with Tamiflu in other all-atom force fields. Due to the united-atom approximation which is responsible for strong conformational changes (Figures 1 and 6) in all systems, the HB network looks differently from other force fields. The thermal fluctuation of each atom of Tamiflu in GROMOS is markedly higher than other force fields. It should be noted that groups $-OCHEt_2$ and $-NH_3^+$ are quite flexible in the AMBER force field. The $OCHEt_2$ group of Tamiflu also fluctuates much upon binding to H274Y (Figure 6) within AMBER and CHARMM.

The situation becomes different if one concerns mutants in GROMOS. The hydrogen bonding between ligand and receptor is even stronger than in the WT case (compare Figure 5 and Figures S7−S9, Supporting Information). For Y252H, HBs mainly connect Tamiflu with E119, R156, R292, and Y347 (>50%), while HB binding with R118 and E119 is strongest (>70%) for N294S. Nevertheless, in GROMOS the HB network remains weak for all studied systems leading to high mobility of Tamiflu within the binding pocket (see also Figure S10, Supporting Information). For the remaining full-atom force fields, the HB network is similar for all variants (Figures S7−S9, Supporting Information).

■ CONCLUSIONS

Having applied the MM-PBSA method and four different force fields to study the binding affinity of Tamiflu to WT and variants of A/H5N1 NA, we have obtained a number of interesting results:

(1) As evident in Figure 4, it is not easy to reproduce experimental results on the quantitative level as binding free energies depend not only on force fields but also on methods we use. However, one can mimic relative binding affinities of Tamiflu to WT and mutants. From this prospect, the OPLS-AA/L is a good example as it provides large negative values of ΔG_{bind} (Table 2) but still maintains the general binding trend Y252H → WT → N294S → H274Y observed in experiments.[25] This ranking is also supported by AMBER and CHARMM.

(2) In this paper the force field validity is justified by contrast of simulation results against the experiments. However, one has to be also careful in interpretation of experimental data because the same group may provide different values of ΔG_{bind} for the same system.[64,65]

(3) For the first time we have theoretically studied the response of mutant Y252H to Tamiflu. In agreement with the experiments,[25] all four force fields support that its binding susceptibility is higher than WT (Tables 1−4). Qualitatively, the notable departure from the experiments has been obtained using the GROMOS96 force field (Table 1). This may be due to short comings of either the united-atom approximation or the MM-PBSA approach. It would be interesting to check if other methods change our conclusion. This question is left for further investigation.

(4) The binding free energies depend not only on force fields but also on computational methods (Figure 4). For example, using the same AMBER99SB but MM-PBSA[30] and FEP[33] gives different values for ΔG_{bind}. In addition, even employing the same method and model, the discrepancy occurs among different groups (Figure 4) pointing to importance of the equilibration problem.

(5) We have performed the simulations at the normal density of water of 1 kg/L. An interesting question emerges, how does water density influence the unbinding free energy. As mentioned in the previous papers,[61,66] water molecules weaken HBs between the ligand and the receptor. As a result, the binding affinity is expected to fall with an increase of the water density. To explicitly show this we have calculated the binding free energy ΔG_{bind} in the absence of water using the AMBER99SB force field. For this case we have $\Delta G_{bind} \approx -41.9$ kcal/mol, which is much lower than $\Delta G_{bind} \approx -13.91$ kcal/mol obtained for the normal TIP3P water concentration of 1 kg/1 L (Table 3).

(6) Recently, it has been shown[61,67,68] that the steered molecular dynamics (SMD) approach[69,70] is a promising tool for drug design. In this approach the ligand is pulled from the binding pocket, and its binding affinity is defined by the maximum force in the force−extension profile. The predictive power of SMD is comparable with that of MM-PBSA, but in terms of computational effort, it is much less expensive. Therefore it would be very appealing to apply this method to explore differences between force fields in the description of ligand binding properties.

■ ASSOCIATED CONTENT

Supporting Information. Additional figures including the detailed description of Tamiflu charges extracted from HF and B3LYP theoretical models, the initial structure for MD simulation, the time dependence of the number of HBs between Oseltamivir and receptors, and typical snapshots of HB networks are presented. Four tables on names and types of atoms and ESP charges used in simulation of Tamiflu by four force fields are provided. This material is available free of charge via the Internet at http://pubs.acs.org.

■ AUTHOR INFORMATION

Corresponding Author
*E-mail: masli@ifpan.edu.pl.

■ ACKNOWLEDGMENT

This work was supported by the Department of Science and Technology of Ho Chi Minh City, Vietnam, and the Ministry of Science and Informatics in Poland (grant no 202-204-234).

■ REFERENCES

(1) Du, Q. S.; Wang, S. Q.; Chou, K. C. Analog inhibitors by modifying oseltamivir based on the crystal neuraminidase structure for treating drug-resistant H5N1 virus. *Biochem. Biophys. Res. Commun.* **2007**, *362*, 525–531.

(2) Mihajlovic, M. L.; Mitrasinovic, P. M. Applications of the ArgusLab4/AScore protocol in the structure-based binding affinity prediction of various inhibitors of group-1 and group-2 influenza virus neuraminidases (NAs). *Mol. Simul.* **2009**, *35*, 311–324.

(3) Mitrasinovic, P. M. Reply to Comment on Another look at the molecular mechanism of the resistance of H5N1 influenza A virus neuraminidase (NA) to oseltamivir (OTV). *Biophys. Chem.* **2009**, *141*, 133–133.

(4) Mihajlovic, M. L.; Mitrasinovic, P. M. Some novel insights into the binding of oseltamivir and zanamivir to H5N1 and N9 influenza virus neuraminidases: a homology modeling and flexible docking study. *J. Serb. Chem. Soc.* **2009**, *74*, 1–13.

(5) Mitrasinovic, P. M. Advances in the Structure-Based Design of the Influenza A Neuraminidase Inhibitors, Current Drug Targets. *Curr. Drug Targets* **2010**, *11*, 315–326.

(6) Mihajlovic, M. L.; Mitrasinovic, P. M. Another look at the molecular mechanism of the resistance of H5N1 influenza A virus neuraminidase (NA) to oseltamivir (OTV). *Biophys. Chem.* **2008**, *136*, 152–158.

(7) Wang, S. Q.; Cheng, X. C.; Dong, W. L.; Wang, R. L.; Chou, K. C. Three new powerful oseltamivir derivatives for inhibiting the neuraminidase of influenza virus. *Biochem. Biophys. Res. Commun.* **2010**, *401*, 188–191.

(8) Rungrotmongkol, T.; Malaisree, M.; Udommaneethanakit, T.; Hannongbua, S Comment on "Another look at the molecular mechanism of the resistance of H5N1 influenza A virus neuraminidase (NA) to oseltamivir (OTV). *Biophys. Chem.* **2009**, *141*, 131–132.

(9) Mitrasinovic, P. M. Comment on Comment on "Another look at the molecular mechanism of the resistance of H5N1 influenza A virus neuraminidase (NA) to oseltamivir (OTV)". *Biophys. Chem.* **2011**, *154*, 102–102.

(10) Mitrasinovic, P. M. On the structure-based design of novel inhibitors of H5N1 influenza A virus neuraminidase (NA). *Biophys. Chem.* **2009**, *140*, 35–38.

(11) Zwanzig, R. High Temperature Equation of State by a Perturbation Method. *J. Chem. Phys.* **1954**, *22*, 1420–1426.

(12) Kirkwood, J. Statistical Mechanics of Fluid Mixtures. *J. Chem. Phys.* **1935**, *3*, 300–313.

(13) Aqvist, J.; Medina, C.; Samuelsson, J. New method for prediction binding affinity in computer-aided drug design. *Protein Eng.* **1994**, *7*, 385–391.

(14) Lee, F. S.; Chu, Z. T.; Bolger, M. B.; Warshel, A. Calculations of antibody-antigen interactions: microscopic and semi-microscopic

evaluation of the free energies of binding of phosphorylcholine analogs to McPC603. *Protein Eng.* **1992**, *5*, 215–228.

(15) Bren, U.; Lah, J.; Bren, M.; Martnek, V.; Florin, J. DNA Duplex Stability: The Role of Preorganized Electrostatics. *J. Phys. Chem. B* **2010**, *114*, 2876–2885.

(16) Kollman, P. A.; Massova, I.; Reyes, C.; Kuhn, B.; Huo, S.; Chong, L.; Lee, M.; Lee, T.; Duan, Y.; Wang, W.; Donini, O.; Cieplak, P.; Srinivasan, J.; Case, D. A.; Cheatham, T. E. Calculating structures and free energies of complex molecules: combining molecular mechanics and continuum models. *Acc. Chem. Res.* **2000**, *33*, 889–897.

(17) Karplus, M.; McCammon, J. A. Molecular dynamics simulations of biomolecules. *Nat. Struct. Biol.* **2002**, *9*, 646–652.

(18) Ponder, J. W.; Case, D. A. Force fields for protein simulations. In *Advances in Protein Chemistry*; Elsevier Academic Press: San Diego, CA, 2003; Vol. 66, pp 27−86.

(19) Nguyen, P. H.; Li, M. S.; Derreumaux, P. Effects of all-atom force fields on amyloid oligomerization: Replica exchange molecular dynamics simulations of the Ab16−22 dimer and trimer. *Phys. Chem. Chem. Phys.* **2011**, *13*, 9778–9788.

(20) Webster, R. G.; Govorkova, E. A. H5N1 influenza-continuing evolution and spread. *N. Engl. J. Med.* **2006**, *355*, 2174–2177.

(21) The Writing Committee of the World Health Organization (WHO) Consulation on Human Influenza A/H5, Avian Influenza A (H5N1) Infection in Humans. *N. Engl. J. Med.* **2005**, *97*, 1374-1385

(22) Moscona, M. D. A. Neuraminidase Inhibitors for Influenza. *N. Engl. J. Med.* **2005**, *353*, 1363–1373.

(23) deJong, M. D.; Thanh, T. T.; Khanh, T. H.; Hien, V. M.; Smith, G. J. D.; Chau, N. V.; Cam, B. V.; Qui, P. T.; Ha, D. Q.; Guan, Y.; Peris, J. M. S.; Hien, T. T.; Farrar., J. Oseltamivir resistance during treatment of influenza A (h5N1) infection. *N. Engl. J. Med* **2005**, *353*, 2667–2672.

(24) Le, Q. M.; Kiso, M.; Someya, K.; Sakai, Y. T.; Nguyen, T. H.; Nguyen, K. H.; Pham, N. D.; Ngyen, H. H.; Yamada, S.; Muramoto, Y.; Horimoto, T.; Takada, A.; Goto, H.; Suzuki, T.; Suzuki, Y.; et al. Avian flu: isolation of drug-resistant H5N1 virus. *Nature* **2005**, *437*, 1108.

(25) Collins, P. J.; Haire, L. F.; Lin, Y. P.; Liu, J. F.; Russell, R. J.; Walker, P. A.; Skehel, J. J.; Martin, S. R.; Hay, A. J.; Gamblin, S. J. Crystal structures of oseltamivir-resistant influenza virus neuraminidase mutants. *Nature* **2008**, *453*, 1258–1261.

(26) Wang, N. X.; Zheng, J. J. Computational studies of H5N1 influenza virus resistance to oseltamivir. *Protein Sci.* **2009**, *18*, 707–715.

(27) Malaisree, M.; Rungrotmongkol, T.; Nunthaboot, N.; Aruksakunwong, O.; Intharathep, P.; Decha, P.; Sompornpisut, P.; Hannongbua, S. Source of oseltamivir resistance in avian influenza H5N1 virus with the H274Y mutation. *Amino Acids* **2009**, *37*, 725–732.

(28) Li, Y.; Zhou, B.; Wang, R. Rational design of Tamiflu derivatives targeting at the open conformation of neuraminidase subtype 1. *J. Mol. Graphics Modell.* **2009**, *28*, 203–219.

(29) Aruksakunwong, O.; Malaisree, M.; Decha, P.; Sompornpisut, P.; Parasuk, V.; Pianwanit, S.; Hannongbua, S. On the lower susceptibility of Oseltamivir to Influenza Neuraminidase subtype N1 than those in N2 and N9. *Biophys. J.* **2007**, *92*, 798–807.

(30) Wang, P.; Zhang, J. Z. H. Selective binding of antiinfluenza drugs and their analogues to 'open' and 'closed' conformations of H5N1 Neuraminidase. *J. Phys. Chem. B* **2010**, *114*, 12958–12964.

(31) Park, J. W.; Jo, W. H. Infiltration of water molecules into the Oseltamivir-binding site of H274Y Neuraminidase mutant causes resistance to Oseltamivir. *J. Chem. Inf. Model.* **2009**, *49*, 2735–2741.

(32) Park, J. W.; Jo, W. H. Computational design of novel, high-affinity neuraminidase inhibitors for H5N1 avian influenza virus. *J. Med. Chem.* **2010**, *45*, 536–541.

(33) Laurenz, M.; Wereszczynski, J.; Amaro, R.; Walker, R.; Roitberg, A.; McCammon, J. Impact of calcium on N1 influenza neuraminidase dynamics and binding free energy. *Proteins* **2010**, *78*, 2523–2532.

(34) van Gunsteren, W.; Billeter, S. R.; Eising, A. A.; Hunenberger, P. H.; Kruger, P.; Mark, A. E.; Scott, W. R. P.; Tironi., I. G. *Biomolecular Simulation: The GROMOS96 Manual and User Guide*; Vdf Hochschulverlag AG an der ETH Zurich: Zurich, 1996.

(35) Jorgensen, W. L.; Maxwell, D.; Tirado-Rives, J. Development and Testing of the OPLS All-Atom Force Field on Conformational Energetics and Properties of Organic Liquids. *J. Am. Chem. Soc.* **1996**, *118*, 11225–11236.

(36) Wang, J.; Cieplak, P.; Kollman, P. A. How weel does restrained electrostatic potential (RESP) model perform in calculating conformational energies of organic and biological molecules. *J. Comput. Chem.* **2000**, *21*, 1049–1074.

(37) MacKerell, J. A. D.; Bashford, D.; Bellott, M.; Dunbrack, J. R. L.; Evanseck, J. D.; Field, M. J.; Fischer, S.; Gao, J.; Guo, H.; Ha, S.; Joseph-McCarthy, D.; Kuchnir, L.; Kuczera, K.; Lau, F. T. K.; Mattos, C.; et al. All-atom empirical potential for molecular modeling and dynamics Studies of proteins. *J. Phys. Chem. B* **1998**, *102*, 3586–3616.

(38) *PyMOL: The PyMOL Molecular Graphics System*, version 1.3; Schrödinger, LLC: Cambridge, MA, 2010.

(39) van Aalten, D. M. F.; Bywater, R.; Findlay, J. B. C.; Hendlich, M.; Hooft, R. W. W.; Vriend, G. PRODRG, a program for generating molecular topologies and unique molecular descriptors from coordinates of small molecules. *J. Comput.-Aided Mol. Des.* **1996**, *10*, 255–262.

(40) Frisch, M. J.; Trucks, G. W.; Schlegel, H. B.; Scuseria, G. E.; Robb, M. A.; Cheeseman, J. R.; Montgomery, J. A., Jr.; Vreven, T.; Kudin, K. N.; Burant, J. C.; Millam, J. M.; Iyengar, S. S.; Tomasi, J.; Barone, V.; Mennucci, B.; Cossi, M.; Scalmani, G.; Rega, N.; Petersson, G. A.; Nakatsuji, H.; Hada, M.; Ehara, M.; Toyota, K.; Fukuda, R.; Hasegawa, J.; Ishida, M.; Nakajima, T.; Honda, Y.; Kitao, O.; Nakai, H.; Klene, M.; Li, X.; Knox, J. E.; Hratchian, H. P.; Cross, J. B.; Bakken, V.; Adamo, C.; Jaramillo, J.; Gomperts, R.; Stratmann, R. E.; Yazyev, O.; Austin, A. J.; Cammi, R.; Pomelli, C.; Ochterski, J. W.; Ayala, P. Y.; Morokuma, K.; Voth, G. A.; Salvador, P.; Dannenberg, J. J.; Zakrzewski, V. G.; Dapprich, S.; Daniels, A. D.; Strain, M. C.; Farkas, O.; Malick, D. K.; Rabuck, A. D.; Raghavachari, K.; Foresman, J. B.; Ortiz, J. V.; Cui, Q.; Baboul, A. G.; Clifford, S.; Cioslowski, J.; Stefanov, B. B.; Liu, G.; Liashenko, A.; Piskorz, P.; Komaromi, I.; Martin, R. L.; Fox, D. J.; Keith, T.; Al-Laham, M. A.; Peng, C. Y.; Nanayakkara, A.; Challacombe, M.; Gill, P. M. W.; Johnson, B.; Chen, W.; Wong, M. W.; Gonzalez, C.; Pople, J. A. *Gaussian 03*, revision C.02; Gaussian, Inc.: Wallingford, CT, 2004.

(41) Bayly, C. I.; Cieplak, P.; Cornell, W. D.; Kollman, P. A. A well-behaved electrostatic potential based method using charge restraints for deriving atomic charges: the RESP model. *J. Phys. Chem.* **1993**, *97*, 10269–10280.

(42) Bren, U.; Hodosek, M.; Koller, J. Development and Validation of Empirical Force Field Parameters for Netropsin. *J. Chem. Inf. Model.* **2005**, *45*, 1546–1552.

(43) Zhang, H. D.; Bren, U.; Kozekov, I. D.; Rizzo, C. J.; Stec, D. F.; Guengerich, F. P. Steric and Electrostatic Effects at the C2 Atom Substituent Influence Replication and Miscoding of the DNA Deamination Product Deoxyxanthosine and Analogs by DNA Polymerases. *J. Mol. Biol.* **2009**, *392*, 251–269.

(44) Silva, A. W. S. D.; Vranken, W. F.; Laue, E. D. ACPYPE - AnteChamber PYthon Parser interfacE; to be submitted

(45) Andre, A. S. T. R.; Bruno, A. C. H.; Ricardo, B. A. MKTOP: a Program for Automatic Construction of Molecular Topologies. *J. Braz. Chem. Soc.* **2008**, *19*, 1433–1435.

(46) Zoete, V.; Cuendet, M. A.; Grosdidier, A.; Michielin, O. SwissParam, a Fast Force Field Generation Tool For Small Organic Molecules; to be submitted.

(47) Darden, T.; York, D.; Pedersen, L. Particle mesh Ewald: An Nlog(N) method for Ewald sums in large systems. *J. Chem. Phys.* **1993**, *98*, 10089–10092.

(48) Hockney, R. W.; Goel, S. P.; Eastwood, J. Quit high resolution computer models of plasma. *J. Comput. Phys.* **1974**, *14*, 148–158.

(49) Berendsen, H. J. C.; Postma, J. P. M.; van Gunsteren, W. F.; Dinola, A.; Haak, J. R. Molecular dynamics with coupling to an external bath. *J. Chem. Phys.* **1984**, *81*, 3684–3690.

(50) Parrinello, M.; Rahman, A. Polymorphic transitions in single crystals: A new molecular dynamics method. *J. Appl. Phys.* **1981**, *52*, 7182–7190.

(51) Hess, B.; Kutzner, C.; van der Spoel, D.; Lindahl, E. GROMACS 4: Algorithms for highly efficient, load-balanced, and scalable molecular simulation. *J. Chem. Theory Comput.* **2008**, *4*, 435–447.
(52) Berendsen, H. J. C.; Postma, J. P. M.; van Gunsteren, W. F.; Hermans, J. *Intermolecular Forces*; Reidel: Dordrecht, the Netherlands, 1981.
(53) Jorgensen, W. L.; Chandrasekhar, J.; Madura, J. D.; Impey, R. W.; Klein, M. L. Comparison of simple potential functions for simulating liquid water. *J. Chem. Phys.* **1983**, *779*, 926–935.
(54) Sharp, K. A.; Honig, B. Electrostatic interactions in macromolecules: theory and applications. *Annu. Rev. Biophys. Bio.* **1990**, *19*, 301–332.
(55) Baker, N. A.; Sept, D.; Joseph, S.; Holst, M. J.; McCammon, J. A. Electrostatics of nanosystems: application to microtubules and the ribosome. *Proc. Natl. Acad. Sci.U.S.A.* **2001**, *98*, 10037–10041.
(56) Shrake, A.; Rupley, J. A. Environment and exposure to solvent of protein atoms-lysozyme and insulin. *J. Mol. Biol.* **1973**, *79*, 351–371.
(57) Sitkoff, D.; Sharp, K. A.; Honig, B. Accurate calculation of hydration free energies using macroscopic solvent models. *J. Phys. Chem.* **1994**, *97*, 1978–1988.
(58) Shanno, D. F. Conditioning of quasi-Newton methods for function minimization. *Math. Comput.* **1970**, *24*, 647–656.
(59) McQuarrie, D. A. *Statistical Thermodynamics*, 2nd ed.; Harper and Row: New York, 1973.
(60) Rungrotmongkol, T.; Udommaneethanakit, T.; Malaisree, M.; Nunthaboot, N.; Intharathep, P.; Sompornpisut, P.; Hannongbua, S. How does each substituent functional group of oseltamivir lose its activity against virulent H5N1 influenza mutants? *Biophys. Chem.* **2009**, *145*, 29–36.
(61) Mai, B. K.; Viet, M. H.; Li, M. S. Top-Leads for Swine Influenza A/H1N1 Virus Revealed by Steered Molecular Dynamics Approach. *J. Chem. Inf. Model.* **2010**, *50*, 2236–2247.
(62) Cornell, W. D.; Ceplak, P.; Bayly, C. I.; Gould, I. R.; Merz, K. M.; Ferguson, D. M.; Spellmeyer, D. C.; Fox, T.; Caldwell, J. W.; Kollman, P. A. A 2nd generation force-filed for the simulation of proteins, nucleic-acids, and organic molecules. *J. Am. Chem. Soc.* **1995**, *117*, 5179–5197.
(63) Udommaneethanakit, T.; Rungrotmongkol, T.; Bren, U.; Frecer, V.; Stanislav, M. Dynamic Behavior of Avian Influenza A Virus Neuraminidase Subtype H5N1 in Complex with Oseltamivir, Zanamivir, Peramivir, and Their Phosphonate Analogues. *J. Chem. Inf. Model.* **2009**, *49*, 2323–2332.
(64) Yamashita, M.; Tomozawa, T.; Kakuta, M.; Tokumitsu, A.; Nasu, H.; Kubo, S. CS-8958, a Prodrug of the New Neuraminidase Inhibitor R-125489, Shows Long-Acting Anti-Influenza Virus Activity. *Antimicrob. Agents Chemother.* **2009**, 53, 186–192.
(65) Kiso, M.; Kubo, S.; Ozawa, M.; Le, Q. M.; Nidom, C. A.; Yamashita, M.; Kawaoka, Y. Efficacy of the New Neuraminidase Inhibitor CS-8958 against H5N1 Influenza Viruses. *PLoS Pathog.* **2010**, *6*, 152–158.
(66) Lu, H.; Schulten, K. The key event in force-induced unfolding of titin's immunoglobulin domain. *Biophys. J.* **2000**, *79*, 51–65.
(67) Colizzi, F.; Perozzo, R.; Scapozza, L.; Recanatini, M.; Cavalli, A. Single-molecule pulling simulations can discern active from inactive enzyme inhibitors. *J. Am. Chem. Soc.* **2010**, *132*, 7361–7371.
(68) Mai, B. K.; Li, M. S. Neuraminidase Inhibitor R-125489 - A Promising Drug for Treating Influenza Virus: Steered Molecular Dynamics Approach. *Biochem. Biophys. Res. Commun.* **2011**, *410*, 688–691.
(69) Isralewitz, B.; Gao, M.; Schulten, K. Steered molecular dynamics and mechanical functions of proteins. *Curr. Opin. Struct. Biol.* **2001**, *11*, 224–230.
(70) Kumar, S.; Li., M. S. Biomolecules under mechanical force. *Phys. Rep.* **2010**, *486*, 1–74.
(71) Perdih, A.; Bren, U.; Solmajer, T. Binding free energy calculations of N-sulphonyl-glutamic acid inhibitors of MurD ligase. *J. Mol. Model.* **2009**, *15*, 983–996.
(72) Brown, K. L.; Bren, U.; Stone, M. P.; Guengerich, F. P. Inherent Stereospecificity in the Reaction of Aflatoxin B-1 8,9-Epoxide with Deoxyguanosine and Efficiency of DNA Catalysis. *Chem. Res. Toxicol.* **2009**, *22*, 913–917.
(73) Amaro, R. E.; Cheng, X.; Ivanov, I.; Xu, D.; McCammon, J. A. Characterizing Loop Dynamics and Ligand Recognition in Human- and Avian-Type Influenza Neuraminidases via Generalized Born Molecular Dynamics and End-Point Free Energy Calculations. *J. Am. Chem. Soc.* **2009**, *131*, 4702–4709.